Analysis of the Impact of Relative Humidity and Mineral Nuclei Mode Aerosols Particle Concentration on the Visibility of Desert Aerosols

Yerima S. U[1], Abdulkarim U. Y[2], Tijjani B. I[3], Gana U. M[3], Sani M[4], Aliyu R[5], Shamsuddeen M. F[6], Khamisu U.Y[7] and Abdulhadi D[8]

[1]Nigerian Meteorological Agency (NIMET), Nnamdi Azikwe International Airport Abuja.
[2]Department of Physics, SaadatuRimi Collage of Education Kano, Kano State, Nigeria.
[3] Department of Physics, Bayero University Kano, Kano State, Nigeria.
[4]Center for Atmospheric Research, National Space Research and Development Agency (NARSDA), Anyigba, Nigeria.
[5]Department of Physics, Kano State University of Science and Technology Wudil, Kano State, Nigeria.
[6]Remedial and General Studies Department, Audu Bako Collage of Agriculture Danbatta, Kano State, Nigeria.
[7]Department of Physics, Faculty of science Federal University Dutse, Jigawa State Nigeria.
[8]Department of Science Laboratory Technologhy, Nuhu Bamalli Polytechnic Zaria, Kaduna State, Nigeria

Corresponding Author: sunusiyerima@yahoo.com

(Received 13 April 2021, Accepted 17 May 2021, Published 06 June 2021)

Abstract

This paper presents the results of the Analysis of the Impact of relative humidity and water-soluble aerosol particle concentrations on the visibility and particle size distribution of desert aerosols based on microphysical properties of desert aerosols. The microphysical properties (the extinction coefficients, volume mix ratios, dry mode radii and wet mode radii) were extracted from Optical Properties of Aerosols and Clouds (OPAC 4.0) at eight relative humidities (00 to 99% RH) and at the spectral range of 0.4-0.8 mm. The concentrations of mineral nuclie component (MINN) were varied to obtain five different models. The angstrom exponent (α), the turbidity (β), the curvature (α_2), humidification factor (γ), the mean exponent of aerosol growth curve (μ) and the mean exponent of aerosol size distributions (ν) were determined from the regression analysis of some standard equations. It was observed that the values of (α) are less than 1 throughout the 5 models which signifies the dominance of coarse mode particles over fine mode particles. It was observed that the curvature (α_2) has both monomodal and bimodal types of distributions all through the 5 models and this signifies the dominance of coarse mode particles with some traces of fine mode particles. The visibility was observed to decrease with the increase in RH and increased with wavelength. The analysis further found that there is an inverse power law relationship between humidification factor, the mean exponent of the aerosol size distribution with the mean exponent of the aerosol growth curve (as the magnitude of (μ) decreases across the five models, the magnitudes of (γ) and (ν) increase, but the magnitude of both (γ) and (ν) increases for a given (μ) across the individual models). The mean exponent of aerosol size distribution (μ) being less than 3 indicate hazy condition of the desert atmosphere.

Keywords: Extinction coefficient, Visibility Enhancement parameter, mean exponent of the aerosol size distribution, humidification factor, mean exponent of the aerosol growth curve.

1. Introduction

Aerosols are liquid or solid particles suspended in the air. They have a direct effects on climate because they scatter and absorb solar and infrared radiation in the atmosphere and greatly degrade visibility[1]. Aerosols also alter warm, ice and cloud formation processes by increasing droplet number concentrations and ice particle concentrations [2].Mineral dust can be transported in large plumes many thousands of kilometers away from their source regions causing changes in the biogeochemical processes of the entire world[3]. being an important source of primary nutrients such as nitrogen, phosphorus or potassium[4]. Mineral dust emissions into the atmosphere have a negative impact on human health, mineral dust can cause an aggravating allergies, respiratory diseases, visibility degradation and eyes infections[5].

Atmospheric mineral dust particles can affect chemical, microphysical, and the visibility of the atmosphere which makes them important when considering both natural and anthropogenic climate effects [6].Mineral dusts absorb and scatter radiation while on the other hand they act as cloud condensation nuclei (CCN) and ice nuclei (IN) leading to cloud formation and growth as well as influencing albedo, persistence, and other cloud properties[7,8]. The aerosol particles uptake moisture when the relative humidity increases, as such are more soaked with water from the surrounding humid air and swell[9]. As the particle size increases the visibility also reduced. Hence, quantitatively, the variation of the particle size distribution of aerosol particles with relative humidity has to be taken into account [10].

In the natural environments the changes in the microphysical and optical properties observed at a given wavelength are signs that measuring conditions have changed. These changes can cause unbalance in the atmosphere by causing decrease in visibility or other harmful effects to man and his environment, it might also be related either to an increase in RH or to a change in the aerosol concentration. These detailed changes are not always available for ambient aerosol [11]. Moreover, the impacts of relative humidity and water-soluble component of dessert aerosols on the visibility of the desert atmosphere can cause harmful effects on human health, visibility degradation, and can also affect signal propagation in communication industry. Hence, there is a need to properly study the effect of varying the concentration and water uptake of the mineral transported nuclei aerosols on visibility of the desert atmosphere.

In this paper the extinction coefficients, volume mix ratios, dry mode radii and wet mode radii of desert aerosols were extracted from OPAC (4.0) at the spectral wavelength of 0.4 to 0.8μm, and at relative humidities of 0, 50, 70, 80, 90, 95, 98 and 99%. From the four components of the aerosols (WASO, MINN, MIAN, MICN), the Mineral transported (nuclei mode, nonspherical) MINN was varied. The parameters were analyzed using excel, SPSS, Origin and some standard formulae and determined the effective hygroscopic growth, humidification factor, visibility enhancement

parameter, visibility, the mean exponent of aerosol growth curve and the mean exponent of aerosol size distribution.

2.0 METHODOLOGY

The Table 1 shows the models components of the compositions of the desert aerosols used to determine the extinction coefficients of the mixture.

Table1: The models used in the simulations of the desert aerosols.

	Model1	Model2	Model3	Modle4	Model5
Comp	No. Den. (cm^{-3})	No. Den. (cm^{-3})	No. Den. (cm^{-3})	No. Den. (cm^{-3})	No. Den. (cm^{-3})
WASO	2000	2000	2000	2000	2000
MINN	289.5	309.5	329.5	349.5	369.5
MIAN	30.5	30.5	30.5	30.5	30.5
MICN	0.142	0.142	0.142	0.142	0.142

An objective measure of visibility is the standard visual range or meteorological range [12].

$$Vis(\lambda) = \frac{3.912}{\sigma_{ext}(\lambda)} \tag{1}$$

Meteorological range refers to the visual range of a black object seen against its surrounding [13]. The visual extinction coefficient $\sigma_{ext}(\lambda)$ is the measure of light scattering and absorbing properties of the atmosphere along the line of sight [14]. To determine the visibility using the extracted extinction coefficient, the variation of the extinction coefficient with wavelength was determined using the inverse power law of extinction coefficient as;

$$\sigma_{ext}(\lambda) = \beta\lambda^{-\alpha} \tag{2}$$

where α and β are known as Angstrom parameters. The index α is the wavelength exponent or Angstrom coefficient and β is the turbidity coefficient representing the amount of aerosols present in the atmosphere in the vertical direction or the total aerosol loading in the atmosphere [13,14].

Substituting equation (2) into (1), the following equation is obtained which is the variation of the visibility with wavelength.

$$Vis(\lambda) = \frac{3.912}{\beta}\lambda^{\alpha} \tag{3}$$

Equation (3) can also be written as

$$ln\left(\frac{Vis_{\lambda}}{3.912}\right) = -ln(\beta) + \alpha\, ln(\lambda) \tag{4}$$

To obtain α (slope) and β (intercept) a regression analysis was performed using an expression derived from the Kaufman (1993) representation of the equation [17].

However, The Angstrom exponent itself varies with wavelength, and a more precise empirical relationship between visibility and wavelength is obtained with a 2nd-order polynomial [9,16,19]

$$ln\left(\frac{Vis_{\lambda}}{3.912}\right) = -ln(\beta) + \alpha_1 ln(\lambda) + \alpha_2\left(ln(\lambda)\right)^2 \tag{5}$$

Here, the coefficient α_2 accounts for a "curvature" often observed in the sun photometry measurements. Some authors have noted that the curvature is also an indicator of the aerosol particle size, with negative curvature indicating aerosol size distributions dominated by the fine mode and positive curvature indicating size distributions with a significant coarse mode contribution [20,23].

Now, to determine the relationship between visibility and relative humidity, enhancement parameter is defined as [10].

$$f(RH,\lambda) = \frac{Vis(RH,\lambda)}{Vis(RH=0,\lambda)} = \left[\frac{1-(RH)}{1-(RH=0)}\right]^{-\gamma} \tag{6}$$

Now taking the natural log of both side we have

$$ln\left(\frac{Vis(RH,\lambda)}{Vis(0,\lambda)}\right) = -\gamma ln(1-RH) \tag{7}$$

Also, γ is given as (Tijjani, 2013)

$$\gamma = \frac{(\upsilon-1)}{\mu} \tag{8}$$

Where γ is the humidification factor representing the dependence of visibility on RH, It arises from the change in the particle size and refractive indices upon humidification [9,24]. The use of γ has an advantage of describing the hygroscopic behavior of visibility in a linear manner over a broad range of RH values, and also implies that particles are deliquesced [27], the γ parameter is dimensionless, and it increases with increase in particle water uptake [9]. μ is defined as the mean exponent of the aerosol growth curve constant, υ as the mean exponent of the aerosol size distribution [10].

Junge have demonstrated the need for using logarithmic range for the interpretation of the mean exponent of the aerosol size distributions [28]. Based on experimental observations, he proposed a power law size distribution function of the form;

$$\frac{dn(r)}{d(logr)} = Cr^{-\upsilon} \tag{9}$$

Where dn(r) is the number of particles with radii between r and r+dr, C is constant depending on the number of particles in one cubic centimeter and the exponent υ determines the mean exponent of aerosol size distribution. As υ values decrease the number of larger particles increases compared to smaller particles [24].

Now, the hygroscopic growth g(*RH*) experienced by a single aerosol particle according to [10] is given by

$$g(RH) = \frac{r(RH)}{r(RH=0)} \tag{10}$$

where *r(RH)* is the radius at RH% and *r(RH=o)* is the radius at 0%RH.

Now, the effective hygroscopic growth of the four components of the aerosols is given as:

$$g_{eff}(RH) = \left(\sum_i x_i g_i^3(RH)\right)^{\frac{1}{3}} \tag{11}$$

where the summation is performed over all compounds present in the particles and x_i represents the respective volume fraction of single aerosol particle concentration and g_i is the hygroscopic growth of the i^{th} aerosol particles using the Zdanovskii-Stokes-Robinson relation [29], and i= 1,2,3,4.

Now, expressing the effective hygroscopic growth in terms of relative humidity we have:

$$g_{eff}(RH) = \left[\frac{1-(RH)}{1-(RH=0)}\right]^{-\frac{1}{\mu}} \tag{12}$$

where μ is defined as the mean exponent of the aerosol growth curve constant as defined in equation (8)

taking the natural log of both side we have:

$$\ln g_{eff}(RH) = -\frac{1}{\mu}\ln(1-RH) \tag{13}$$

Now, expressing υ (the mean exponent of the aerosol size distribution) in terms of μ and γ (the humidification factor) using equations (8) and (11) we have:

$$\upsilon = \gamma\mu + 1 \tag{14}$$

3.0 RESULTS AND DISCUSSION

This section presents the results of the analyzed data extracted from OPAC 4.0 based on the models presented in table 1.

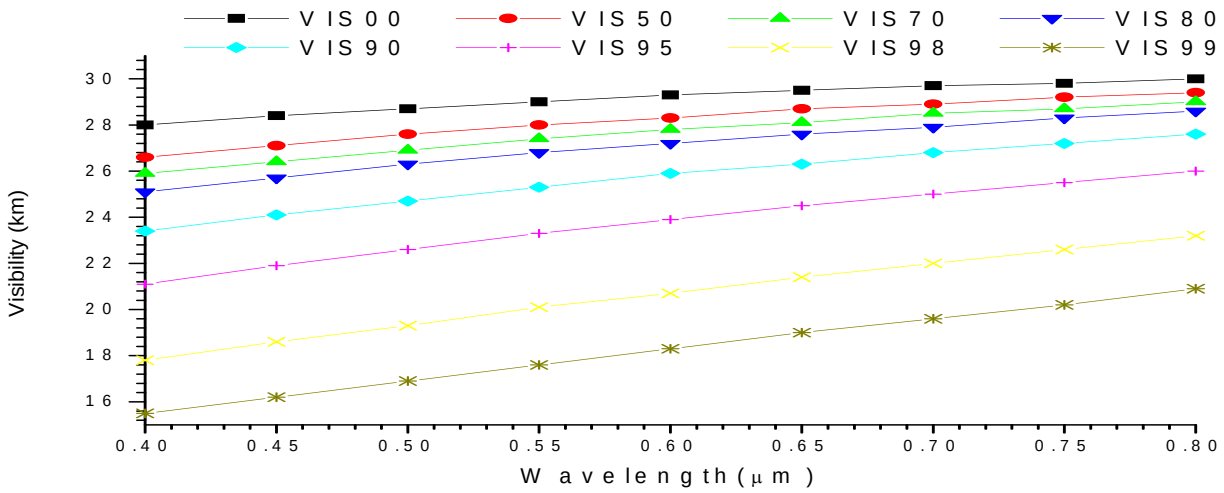

Figure 1 Plot of visibility against wavelengths for minn model 1

From fig. 1, it can be observed that the visibility increases with the increase in wavelength, and decreases with the increase in relative humidity (RH). It can also be observed that the visibility is lower at shorter wavelengths with maximum and minimum values of 23.4km and 13.9km respectively. This shows the dominance of coarse mode particles with some traces of fine mode particles. It should also be noted that fine mode particles scatter and absorb more solar radiation than the coarse mode particles [30]. Since from equation (3) the visibility is the inverse of extinction, this

implies that the visibility will be lower at shorter wavelengths. The change in visibility is more pronounced from 90%RH to 99%RH.

Table 2 Results of the regression analysis of equations (4) and (5) for visibility using SPSS.

	Linear			Quadratic			
RH	R^2	α	β	R^2	α_1	α_2	β
0%	0.992800	0.102978	0.127087	0.992868	0.107839	0.004311	0.126941
50%	0.996747	0.142122	0.128528	0.996998	0.129242	-0.01142	0.128922
70%	0.992636	0.156605	0.130402	0.997725	0.092623	-0.05674	0.132397
80%	0.997639	0.192607	0.130643	0.997679	0.185692	-0.00613	0.130857
90%	0.996251	0.234090	0.134475	0.997424	0.188254	-0.04065	0.135946
95%	0.996276	0.299927	0.140320	0.996549	0.271618	-0.02511	0.141266
98%	0.998768	0.376534	0.155441	0.999064	0.413540	0.032819	0.154082
99%	0.998109	0.424610	0.171760	0.998910	0.493203	0.060832	0.168987

From Table 2, the R^2 values from both linear and quadratic parts shows that the data fitted the equation model very well. From the linear part, since α is less than 1, it signifies the dominance of coarse mode particles, but the magnitude of the α values shows that there are some traces of fine mode particles. the increase of α with increase in RH shows that coarse mode particles are being removed from the atmosphere more than fine mode particles as a result of coagulation and sedimentation due to increase in RH. From the quadratic part, it can be seen that $\alpha_2$is positive at 00%, 98% and 99%RH respectively which shows its bimodal distribution of coarse mode particles. It can also be seen that from 50 to 95% RH it is negative which shows monomodal type of distribution of coarse mode particles. The increase in turbidity coefficient β with RH also signifies that the particles uptake water and swell, which then lead to the decrease in visibility.

Table 3 the result of the analysis of equations (7) and (15) using SPSS.

	μ	12.58748	
λ	R^2	γ	v
0.55	0.952058	0.089219	2.123043
0.65	0.942307	0.077194	1.971678
0.75	0.934438	0.066949	1.842719

By observing the values of R^2 from Table 3, it can be said that the data fitted the equation models very well. Equation (6) shows that the visibility satisfies the inverse power law with (1-RH). The decrease of humidification factor with wavelength also shows that the visibility increases with the increase in wavelength. Equation (12) shows that the hygroscopic growth also satisfied the inverse power relation with (1-RH) and the reciprocal of mean exponent of aerosol growth curve. It can also be said that for a fixed value of mean exponent of the aerosol growth curve μ, the humidification factor γ decreases with the increase in wavelength, this also shows that the visibility increases with

the increase in wavelength (as the particles size decreases) i.e it satisfies the inverse power law of equation (6) and decreases with an increase in RH. Based on equation (9), the mean exponent of the aerosol size distribution (v) decrease with the increase in wavelength which shows that the number of larger particles increase compared to smaller particles and this is due to major coagulation amount caused by the increase in number of fine mode particles and consequently the tiny particles coagulate more than the larger particles as said by [28] and [9]. It can also be noted from the values of (v) that the average atmospheric condition of the area is foggy [28].

Table 4 Results of the analysis of skewness and kurtosis using SPSS.

	lnvis00	lnvis50	lnvis70	lnvis80	lnvis90	lnvis95	lnvis98	lnvis99
Skewness	-0.2683	-0.3688	-0.5464	-0.3286	-0.4181	-0.3588	-0.2568	-0.2260
Kurtosis	-1.2939	-0.9361	-0.7396	-1.1790	-1.0478	-1.1757	-1.1487	-1.2045

From Table 4, the behaviors and changes of particles size distribution are displayed in terms of vertical behavior (kurtosis) and horizontal behavior (skewness). From skewness, it can be seen that it is negative from the visibility of 00 to 99%, this implies that it is negatively skewed and this signifies that the particle distribution is dominated by coarse mode particles. From the kurtosis, it can be observed that it is also negative all through. and this shows that it is platykurtic, and the average vertical size distribution of the particles is below normal size distribution. The fluctuations in the values of the values of skewness and kurtosis maybe due to the nonlinear relation between the particles size distribution with RH and the physically mixed aerosols.

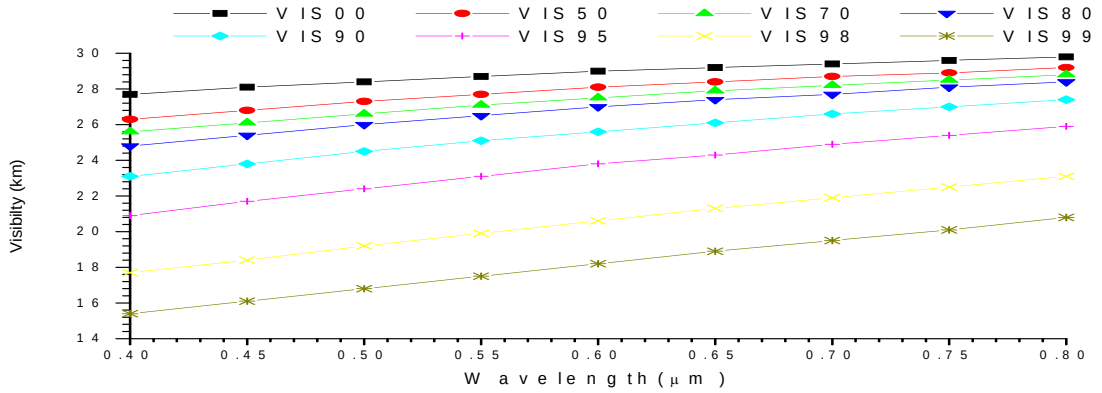

Figure 2 plot of visibility against wavelengths for minn model 2

From fig. 2, it can be observed that the visibility increases with the increase in wavelength, and decreases with the increase in relative humidity (RH). It can also be observed that the visibility is lower at shorter wavelengths which shows the dominance of coarse mode particles with some traces of fine mode particles. It should also be noted that fine mode particles scatter and absorb more solar radiation than the coarse mode particles [30]. Since from equation (3) the visibility is the inverse of extinction, this implies that the visibility will be lower at shorter wavelengths.

Table 5 Results of the regression analysis of equations (4) and (5) for visibility using SPSS.

	Linear			Quadratic			
RH	R^2	α	β	R^2	α_1	α_2	β
0%	0.992855	0.102978	0.128364	0.992868	0.107839	0.004311	0.128216
50%	0.996747	0.142122	0.12982	0.996998	0.129242	-0.01142	0.130217
70%	0.996306	0.173166	0.130116	0.996397	0.163711	-0.00839	0.130408
80%	0.995291	0.194945	0.131644	0.995926	0.166851	-0.02492	0.132525
90%	0.997992	0.245100	0.134729	0.998024	0.237081	-0.00711	0.134986
95%	0.998486	0.305525	0.140993	0.998587	0.288061	-0.01549	0.141578
98%	0.999404	0.380672	0.156308	0.999505	0.402532	0.019387	0.155578
99%	0.998569	0.438166	0.171278	0.999364	0.508693	0.062547	0.168435

From Table 5, observing the R^2 values from both linear and quadratic parts, it can be seen that the data fitted the equation model very well. From the linear part, it can be seen thatα is less than 1, which signifies the dominance of coarse mode particles, but the increase in the magnitude of α with the increase in RHsignifies that coarse mode particles are removed from the atmosphere more than fine mode particles as a result of coagulation and sedimentation. From the quadratic part, it can be seen that α_2 is positive at 00, 98 and 99%RH respectively, which shows its bimodal type of distribution.It can also be seen that it is negative from 50 to 95% RH which signifiesmonomodal type of distribution. The fluctuations in the values of α_2 is due to coagulation and sedimentation. the increase in turbidity coefficient β with RH also signifies the particles swelled up due to water uptake and cause the decrease in visibility.

Table 6 the result of the analysis of equations (8) and (12) using SPSS.

	μ	12.60414	
λ	R^2	γ	v
0.55	0.951854	0.088453	2.114874
0.65	0.943029	0.076800	1.967998
0.75	0.933635	0.066459	1.837659

Observing R^2 the values from Table 6, it can be said that the data fitted the equation models very well. Equation (6) shows that the visibility satisfies the inverse power law with (1-RH). The decrease of humidification factor with wavelength also shows that the visibility increases with the increase in wavelength. Equation (12) shows that the hygroscopic growth also satisfied the inverse power relation with (1-RH) and the reciprocal of mean exponent of aerosol growth curve. It can also be said that for a fixed value of mean exponent of the aerosol growth curve μ, the humidification factor γ decreases with the increase in wavelength, this also shows that the visibility increases with the increase in wavelength (as the particles size decreases) i.e it satisfies the inverse power law of equation (6) and decreases with an increase in RH. Based on equation (9), the mean exponent of the aerosol size distribution (v) decrease with the increase in wavelength which shows that the number

of larger particles increase compared to smaller particles and this is due to major coagulation amount caused by the increase in number of fine mode particles and consequently the tiny particles coagulate more than the larger particles as said by [28] and [9]. It can also be noted from the values of (v) that the average atmospheric condition of the area is foggy [28].

Table 7 the results of the analysis of skewness and kurtosis using SPSS.

	lnvis00	lnvis50	lnvis70	lnvis80	lnvis90	lnvis95	lnvis98	lnvis99
Skewness	-0.2683	-0.3688	-0.3392	-0.3828	-0.3293	-0.3470	-0.2799	-0.2239
Kurtosis	-1.2939	-0.9361	-0.9543	-1.2706	-1.0953	-1.0416	-1.1139	-1.1518

From Table 7, the behaviors and changes of particles size distribution are displayed in terms of vertical behavior (kurtosis) and horizontal behavior (skewness). From skewness, it can be seen that it is negative from the visibility of 00 to 99%, this implies that it is negatively skewed and this signifies that the particle distribution is dominated by coarse mode particles. From the kurtosis, it can be observed that it is also negative all through the RHs, and this shows that it is platykurtic, and the average vertical size distribution of the particles is below normal size distribution. The fluctuations in the values of skewness and kurtosis maybe due to the nonlinear relation between the particles size distribution with RH and the physically mixed aerosols.

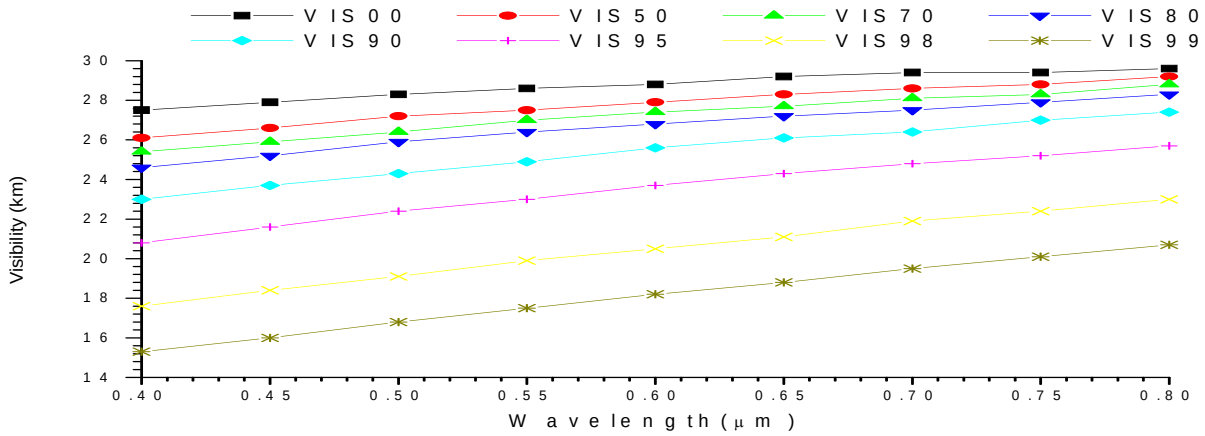

Figure 3 plot of visibility against wavelengths for minn model 3

From figure 3, it can be observed that the visibility increases with an increase in wavelength and decreases with the increase in RH. It should be noted that the relationship between the change in visibility with RH is nonlinear. It can also be observed that the visibility is lower at shorter wavelengths which shows the dominance of coarse mode particles with some traces of fine mode particles. It should also be noted that fine mode particles scatter and absorb more solar radiation than the coarse mode particles [30]. and this shows that there is more visibility reduction caused by fine mode particles than coarse mode particles. More so, the rate of increase in visibility with RHs is more pronounced as from 90-99% RHs.

Table 8 Results of the regression analysis of equations (4) and (5) for visibility using SPSS.

	Linear			Quadratic			
RH	R^2	α	β	R^2	α_1	α_2	β
0%	0.968502	0.104523	0.128544	0.988489	0.018847	-0.07598	0.131184
50%	0.996531	0.158017	0.129150	0.997796	0.125891	-0.02849	0.130139
70%	0.981881	0.182514	0.130478	0.996240	0.194580	0.010701	0.130104
80%	0.995080	0.202547	0.131840	0.995451	0.180222	-0.01980	0.132541
90%	0.995248	0.249984	0.135126	0.997320	0.184902	-0.05772	0.137229
95%	0.995690	0.306478	0.141706	0.997335	0.235409	-0.06303	0.144116
98%	0.997331	0.380080	0.156880	0.998064	0.438872	0.052140	0.154707
99%	0.998002	0.428616	0.172538	0.998576	0.487315	0.052059	0.170152

From Table 8, observing the R^2 values from both linear and quadratic parts, it can be seen that the data fitted the equation models very well. From the linear part, since α is less than 1, this signifies the dominance of coarse mode particles over fine mode particles.But the values ofα increases with the increase in RH which shows that coarse mode particles are removed from the atmosphere more than fine mode particles as a result of sedimentationdue to water uptake by the aerosol particles. From the quadratic part, it can be seen that α_2 is positiveat70%, 98%and99% RH respectively which shows that it is bimodal type of distribution.It can also be seen that it is negative from 00% to 50%RH and from 80% to 95%RH, and this signifies that it is monomodal type of distribution.The fluctuation between the magnitude, positive and negative in α_2 is due to coagulation and sedimentation. The increase in turbidity coefficient β with RH also signifies that the particles uptake water and swelled, which lead to thedecrease in visibility.

Table 9 the result of the analysis of equations (8) and (12) using SPSS.

	μ	12.60637	
λ	R^2	γ	v
0.55	0.951666	0.087924	2.108402
0.65	0.945881	0.077633	1.97867
0.75	0.929498	0.065735	1.828679

From Table 9, observing the values of R^2, it can be said that the data fitted the equation models very well. Equation (6) shows that the visibility satisfies the inverse power law with (1-RH). The decrease of humidification factor with wavelength also shows that the visibility increases with the increase in wavelength. Equation (12) shows that the hygroscopic growth also satisfied the inverse power relation with (1-RH) and the reciprocal of mean exponent of aerosol growth curve. It can also be said that for a fixed value of mean exponent of the aerosol growth curve μ, the humidification factor γ decreases with the increase in wavelength, this also shows that the visibility increases with the increase in wavelength (as the particles size decreases) i.e it satisfies the inverse power law of equation (6) and decreases with an increase in RH. Based on equation (9), the mean exponent of the

aerosol size distribution (v) decrease with the increase in wavelength which shows that the number of larger particles increase compared to smaller particles and this is due to major coagulation amount caused by the increase in number of fine mode particles and consequently the tiny particles coagulate more than the larger particles as said by [28] and [9]. It can also be noted from the values of (v) that the average atmospheric condition of the area is foggy [28].

Table 10 The results of the analysis of skewness and kurtosis using SPSS.

	lnvis00	lnvis50	lnvis70	lnvis80	lnvis90	lnvis95	lnvis98	lnvis99
Skewness	-0.6973	-0.4274	-0.2629	-0.3766	-0.4493	-0.4309	-0.2296	-0.2318
Kurtosis	-0.5560	-0.9375	-0.9464	-0.9036	-1.0372	-1.0741	-1.2595	-1.0428

From Table 10, the behaviors and changes of particles size distribution are displayed in terms of vertical behavior (kurtosis) and horizontal behavior (skewness). From skewness, it can be seen that it is negative from the visibility of 00 to 99%, this implies that it is negatively skewed and this signifies that the particle distribution is dominated by coarse mode particles. From the kurtosis, it can be observed that it is also negative all through, and this shows that it is platykurtic, and the average vertical size distribution of the particles is below normal size distribution. The fluctuations in the values of skewness and kurtosis maybe due to the nonlinear relation between the particles size distribution with RH and the physically mixed aerosols.

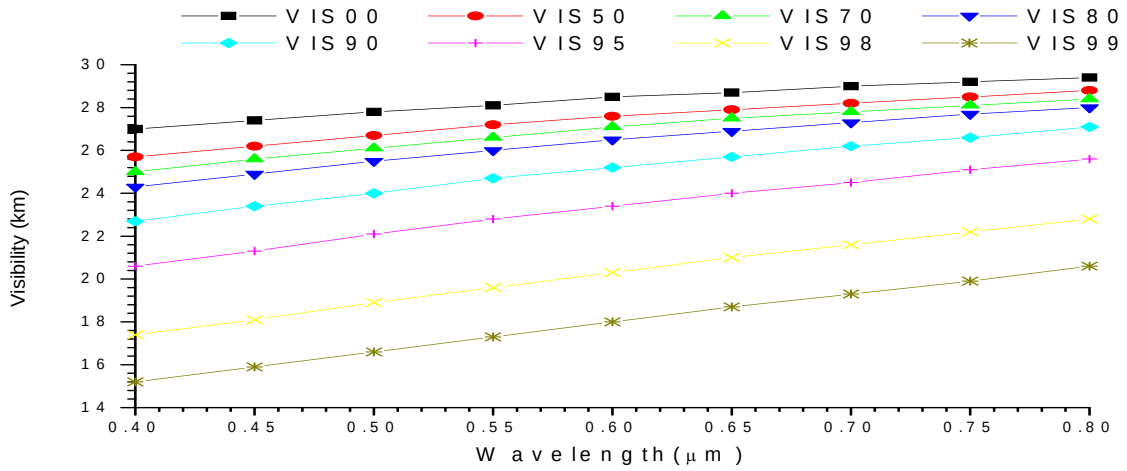

Figure 4 plot of visibility against wavelengths for minn model 4

From figure 4, it can be observed that the visibility increases with the increase in wavelength, and decreases with the increase in relative humidity (RH). It can also be observed that the visibility is lower at shorter wavelengths with maximum and minimum values of 23.4km and 13.9km respectively. This shows the dominance of coarse mode particles with some traces of fine mode particles. It should also be noted that fine mode particles scatter and absorb more solar radiation than the coarse mode particles [30]. Since from equation (3) the visibility is the inverse of extinction, this

implies that the visibility will be lower at shorter wavelengths. The change in visibility is more pronounced from 90%RH to 99%RH.

Table 11 Results of the regression analysis of equations (4) and (5) for visibility using SPSS.

	Linear			Quadratic			
RH	R^2	α	β	R^2	α_1	α_2	β
0%	0.9952	0.1241	0.1293	0.9958	0.1405	0.0146	0.1288
50%	0.9969	0.1465	0.1298	0.9979	0.1449	-0.0272	0.1308
70%	0.9923	0.1841	0.1320	0.9978	0.1056	-0.0696	0.1345
80%	0.9947	0.2146	0.1326	0.9963	0.1663	-0.0429	0.1341
90%	0.9986	0.2471	0.1370	0.9987	0.2340	-0.0116	0.1374
95%	0.9992	0.3167	0.1422	0.9993	0.3262	0.0084	0.1419
98%	0.9989	0.4001	0.1569	0.9990	0.4245	0.0216	0.1560
99%	0.9986	0.4382	0.1730	0.9994	0.5087	0.0625	0.1701

From Table11, it can be seen that the R^2 values from both linear and quadratic parts fitted the equation models very well. From the linear part, since α is less than 1, it signifies the dominance of coarse mode particles with some traces of fine mode particles. it can also be noted that the magnitude ofα increases with the increase in RH, which shows that coarse mode particles are removed from the atmosphere more than fine mode particles as a result of coagulation and sedimentation. From the quadratic part, it can be seen that α_2 is positive at 00% and from 95% to 99%RH, which shows that it is bimodal type of distribution. It can also be seen that it is negative from 50% to 90% RH and this signifies that it is monomodal type of distribution.The increase in the magnitude of the turbidity coefficient β with RH also signifies that the visibility decreased due to water uptake as a result of the change in relative humidity.

Table 12 the result of the analysis of equations (8) and (12) using SPSS.

	μ	12.63695	
λ	R^2	γ	v
0.55	0.951105	0.08691	2.098278
0.65	0.941806	0.075499	1.954077
0.75	0.934048	0.065729	1.830614

By observing the values of R^2 in Table 12, it can be said that the data fitted the equation models very well. Equation (6) shows that the visibility satisfies the inverse power law with (1-RH). The decrease of humidification factor with wavelength also shows that the visibility increases with the increase in wavelength. Equation (12) shows that the hygroscopic growth also satisfied the inverse power relation with (1-RH) and the reciprocal of mean exponent of aerosol growth curve. It can also be said that for a fixed value of mean exponent of the aerosol growth curve μ, the humidification factor γ decreases with the increase in wavelength, this also shows that the visibility increases with the increase in wavelength (as the particles size decreases) i.e it satisfies the inverse power law of

equation (6) and decreases with an increase in RH. Based on equation (9), the mean exponent of the aerosol size distribution (v) decrease with the increase in wavelength which shows that the number of larger particles increase compared to smaller particles and this is due to major coagulation amount caused by the increase in number of fine mode particles and consequently the tiny particles coagulate more than the larger particles as said by [28] and [9]. It can also be noted from the values of (v) that the average atmospheric condition of the area is foggy [28].

Table 13 the results of the analysis of skewness and kurtosis using SPSS.

	lnvis00	lnvis50	lnvis70	lnvis80	lnvis90	lnvis95	lnvis98	lnvis99
Skewness	-0.2418	-0.4062	-0.5602	-0.4399	-0.3403	-0.2949	-0.2793	-0.2239
Kurtosis	-0.7605	-1.0516	-0.6429	-0.8426	-0.9691	-1.0302	-1.2170	-1.1518

From Table 13, it can be observed that the behaviors and changes of particles size distribution are displayed in terms of vertical behavior (kurtosis) and horizontal behavior (skewness). From the skewness, it can be seen that it is negative from the visibility of 00 to 99%, this implies that it is negatively skewed and this signifies that the particle distribution is dominated by coarse mode particles. From the kurtosis, it can be observed that it is also negative all through, and this shows that it is platykurtic, and the average vertical size distribution of the particles is below normal size distribution. The fluctuations in the values of skewness and kurtosis maybe due major coagulation and the nonlinear relation between the particles size distribution with RH and the physically mixed aerosols.

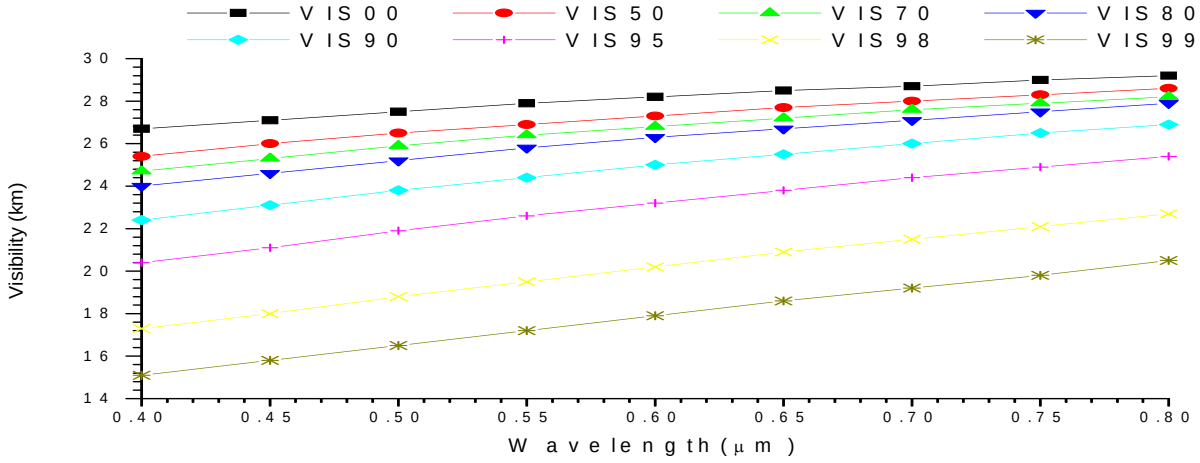

Figure 5 plot of visibility against wavelengths for minn model 5

From figure 5, it can be seen that the visibility increased with the increase in wavelength, and decreases with the increase in relative humidity (RH). It can also be observed that the change is small from 00% to 80% RH compared to 90% to 99%RH. The change in visibility shows that the relationship between RH and the Visibility is nonlinear. It can also be observed that the visibility is lower at shorter wavelength and this can be attributed to the fact that fine mode particles scatter and

absorb more solar radiation than the coarse mode particles [30]. Since from equation (3) the visibility is the inverse of extinction, this implies that the visibility will be lower at shorter wavelengths.

Table 14 Results of the regression analysis of equations (4) and (5) for visibility using SPSS.

	Linear			Quadratic			
RH	R^2	α	β	R^2	α_1	α_2	β
0%	0.988454	0.126432	0.130334	0.988497	0.121688	-0.00421	0.130481
50%	0.996943	0.175504	0.131113	0.997876	0.144870	-0.02717	0.132070
70%	0.995546	0.196620	0.132112	0.995834	0.177559	-0.01690	0.132711
80%	0.994615	0.218649	0.133498	0.996427	0.165390	-0.04723	0.135196
90%	0.997157	0.256995	0.137187	0.997389	0.234613	-0.01985	0.137918
95%	0.999150	0.319039	0.143282	0.999191	0.307380	-0.01034	0.143679
98%	0.999221	0.396237	0.158143	0.999276	0.412962	0.014833	0.157517
99%	0.997855	0.447515	0.173480	0.999152	0.539562	0.081633	0.169732

From Table 14, observing the R^2 values from both linear and quadratic parts, it can be seen that the data fitted the equation models very well. From the linear part, since α is less than 1, and this signifies the dominance of coarse mode particles with some traces of fine mode particles, but since the magnitude of α increase with an increase in RH, this also shows that coarse mode particles are removed from the atmosphere more than fine mode particles as a result of coagulation and sedimentation. From the quadratic part, it can be seen that α_2 is negative from 00 to 95% RH which shows its monomodal coarse mode type of distribution. It can also be seen that it is positive from 98 to 99% RH which shows bimodal type of distribution. the increase in turbidity coefficient β with RH also signifies decrease in visibility.

Table 15the result of the analysis of equations (8) and (12) using SPSS.

	μ	12.65534	
Λ	R^2	γ	v
0.55	0.950909	0.086183	2.090676
0.65	0.942535	0.075125	1.950733
0.75	0.938431	0.065604	1.830241

From Table 15, by observing the values of R^2, it can be said that the data fitted the equation models very well. Equation (6) shows that the visibility satisfies the inverse power law with (1-RH). The decrease of humidification factor with wavelength also shows that the visibility increases with the increase in wavelength. Equation (12) shows that the hygroscopic growth also satisfied the inverse power relation with (1-RH) and the reciprocal of mean exponent of aerosol growth curve. It can also be said that for a fixed value of mean exponent of the aerosol growth curve μ, the humidification factor γ decreases with the increase in wavelength, this also shows that the visibility increases with the increase in wavelength (as the particles size decreases) i.e it satisfies the inverse

power law of equation (6) and decreases with an increase in RH. Based on equation (9), the mean exponent of the aerosol size distribution (v) decrease with the increase in wavelength which shows that the number of larger particles increase compared to smaller particles and this is due to major coagulation amount caused by the increase in number of fine mode particles and consequently the tiny particles coagulate more than the larger particles as said by [28] and [9]. It can also be noted from the values of (v) that the average atmospheric condition of the area is foggy [28].

Table 16the results of the analysis of skewness and kurtosis using SPSS.

	lnvis00	lnvis50	lnvis70	lnvis80	lnvis90	lnvis95	lnvis98	lnvis99
Skewness	-0.3214	-0.4062	-0.3701	-0.4445	-0.3567	-0.3322	-0.2870	-0.1968
Kurtosis	-0.9603	-1.0516	-0.7258	-0.9576	-0.9914	-1.0904	-0.9197	-1.1413

From Table 16, it can be seen that the behaviors and changes of particles size distribution are displayed in terms of vertical behavior (kurtosis) and horizontal behavior (skewness). From the skewness (vertical behavior), it can be seen that it is negative from the visibility of 00 to 99%, this implies that it is negatively skewed and this signifies that the particle distribution is dominated by coarse mode particles. From the kurtosis (horizontal behavior), it can be observed that it is also negative all through, and this signifies that it is platykurtic, and the average vertical size distribution of the particles is below normal size distribution. The fluctuations in the values of skewness and kurtosis maybe due to major coagulation and the nonlinear relation between the particles size distribution with RH and the physically mixed aerosols.

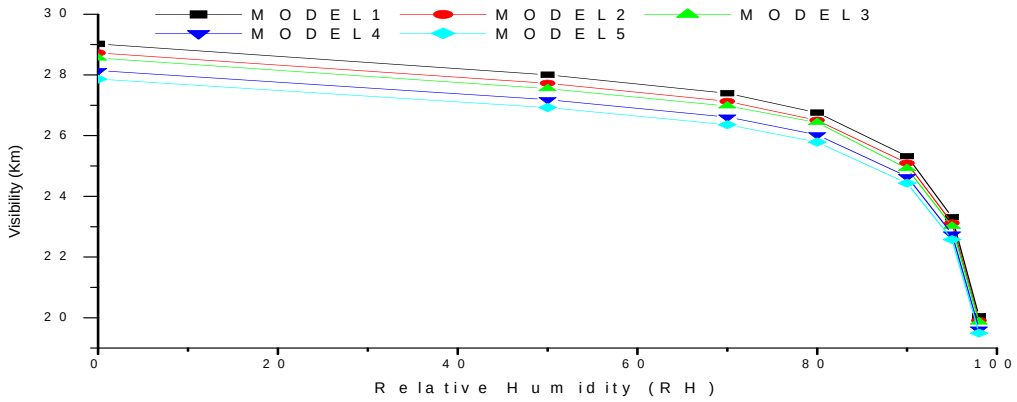

Fig. 6 plot of Visibility against Relative Humidity (RH%) at 0.55µm spectral wavelength (green) and varrying MINN concentrartion

It can be observed from fig. 6 that the visibility decrease with the increase in MINN concentrations and also decresease with the increase in RH across the five models.

4. Summary

From the models considered, it was observed that

I. the (α) angstrom exponent values are less than 1 throughout and increased with the increase in RHs and aerosols concentrations.

II. The curvature (α_2)is be observed to be monomodal type of distribution from 50 to 95% RH and bimodal distribution at 00, 98 and 99%RH for models 1,2 and 4. It can also be observed that the distribution is monomodal from 0 to 95% RH and bimodal at 98 and 99% RH for models3 and 5 respectively.

III. It can be observed that the turbidity coefficients β increase with the increase in RH across all the models, this implies that the visibility decreases with the increase in RH.

IV. Based on the results of the analysis of equations (6), (9), (12) and the plots of visibility against the wavelengths, it can be observed that there is an inverse relation between the humidification factor γ, the mean exponent of the aerosol size distribution v with the particles concentration (i.e as the magnitudes of the humidification factor and the mean exponent of aerosol size distribution decrease with the increase in the concentration of the particles and the increase in wavelengths across the models, the visibility decreases across the models). It can also be observed that as the magnitude of the mean exponent of aerosol growth curve (μ) increase with the increase in particles concentration and the increase of wavelengths across the models, the magnitudes of the humidification factor (γ) and the mean exponent of aerosol size distribution (v) decreased across the models which signifies the direct inverse relation between them.

V. It can be observed that there are fluctuations in the magnitude of the skewness and kurtosis across the studied models. This may be due to the nonlinear relationship between the particle size distribution and the physically mixed aerosols with RH.

5. Conclusion

So, it can be concluded that, the visibility decreases with the increase in RHs, increase in MINN (particles concentration) and with the increase in wavelengths. Also, the increase in the magnitude of the values of (α) across the models and at all RHs implied coarse mode particles. the fluctuations of (α_2) as a result of the change in RHs and particle concentrations signifies nonlinear relationship between RHs and the physically mixed aerosols. It can also be concluded that the visibility decreased with the increase in the magnitudes of both the humidification factor (γ) and the mean exponent of aerosol size distribution (v). There is a direct relationship between the mean exponent of aerosol size distribution, the humidification factor with the mean exponent of aerosol growth curve. Additionally, the fluctuations in the magnitude of skewness and kurtosis also signifies that there is dominance of coarse mode particles with some traces of fine mode particles across the models and that the relationship between the particles size distribution, RHs with the physically mixed aerosols is nonlinear.

Reference

[1] P. Zieger, R. Fierz-Schmidhauser, E. Weingartner, and U. Baltensperger, "Effects of relative humidity on aerosol light scattering : Results from different European sites" *Atmos. Chem. Phys.*, 13, 10609–10631, 2013

[2] D. J. Jacob, J. M. Waldman, J. W. Munger, and M. R. Hoffmann, "The H2SO4- HNO3- NH3 system at high humidities and in fogs. 2. Comparison of field data with thermodynamic calculations.," *J. Geophys. Res.*, vol. 91, no. D1, pp. 1089–1096, 1986

[3] B. A. Maher, J. M. Prospero, D. Mackie, D. Gaiero, P. P. Hesse, and Y. Balkanski, "Global connections between aeolian dust, climate and ocean biogeochemistry at the present day and at the last glacial maximum," *Earth-Science Rev.*, vol. 99, no. 1–2, pp. 61–97, 2010

[4] T. D. Jickells *et al.*, "Global iron connections between desert dust, ocean biogeochemistry, and climate," *Science (80-.).*, vol. 308, no. 5718, pp. 67–71, 2005

[5] C. A. Kellogg and D. W. Griffin, "Aerobiology and the global transport of desert dust," *Trends Ecol. Evol.*, vol. 21, no. 11, pp. 638–644, 2006

[6] H. Herich *et al.*, "Water uptake of clay and desert dust aerosol particles at sub- and supersaturated water vapor conditions," *Phys. Chem. Chem. Phys.*, vol. 11, no. 36, pp. 7804–7809, 2009

[7] R. T. Sataloff, M. D. Johns, and K. M. Kost, "Climate: The Influence of Aerosols on climate," vol. 8, no. 1, pp. 451–456, 1969.

[8] C. Camino *et al.*, "An empirical equation to estimate mineral dust concentrations from visibility observations in Northern Africa," *Aeolian Res.*, vol. 16, no. July 2018, pp. 55–68, 2015

[9] R. Lang and N. X. Xanh, "Smoluchowski's theory of coagulation in colloids holds rigorously in the Boltzmann-Grad-limit," *Zeitschrift für Wahrscheinlichkeitstheorie und Verwandte Gebiete*, vol. 54, no. 3, pp. 227–280, 1980

[10] F. Kasten, "Visibility forecast in the phase of pre-condensation," *Tellus*, vol. 21, no. 5, pp. 631–635, Jan. 1969

[11] B. I. Tijjani, F. Sha'aibu, and A. Aliyu, "The Effect of Relative Humidity on Maritime Tropical Aerosols," *Open J. Appl. Sci.*, vol. 04, no. 06, pp. 299–322, 2014

[12] P. Tsilimigras, "On the applicability of the Roothaan-Bagus procedure," *Chem. Phys. Lett.*, vol. 11, no. 1, pp. 99–100, 1971

[13] R. J. Charlson, "current research," vol. 3, no. 10, pp. 913–918, 1969.

[14] and I. schult M. Hess, P. Koepke, "Optical Properties of Aerosols and Clouds: The Software Package OPAC," pp. 831–844, 1998.

[15] K. K. Moorthy, A. Saha, B. S. N. Prasad, K. Niranjan, D. Jhurry, and P. S. Pillai, "Aerosol optical depths over peninsular India and adjoining oceans during the INDOEX campaigns: Spatial, temporal, and spectral characteristics," *J. Geophys. Res. Atmos.*, vol. 106, no. D22, pp. 28539–28554, 2001

[16] S. Singh, S. Nath, R. Kohli, and R. Singh, "Aerosols over Delhi during pre-monsoon months : Characteristics and effects on surface radiation forcing," *Geophys. Res. Lett.*, vol. 32, no. 1, pp. 4–7, 2005

[17] E. L. Koschmieder, "Symmetric Circulations of Planetary Atmospheres," *Adv. Geophys.*, vol. 20, no. C, pp. 131–181, 1978

[18] M. D. and D. M. B. King, "A method for inferring total ozone content from spectral variation of total optical depth obtained with solar radiometer." pp. 2242–2251, 1976.

[19] B. I. Tijjani, F. Sha'aibu, and A. Aliyu, "The Effect of Relative Humidity on Maritime Polluted Aerosols," *Open J. Appl. Sci.*, vol. 04, no. 06, pp. 299–322, 2014

[20] N. T. O'Neill, O. Dubovik, and T. F. Eck, "Modified Ångström exponent for the characterization of submicrometer aerosols," *Appl. Opt.*, vol. 40, no. 15, p. 2368, 2001

[21] N. T. O'Neill, T. F. Eck, A. Smirnov, B. N. Holben, and S. Thulasiraman, "Spectral discrimination of coarse and fine mode optical depth," *J. Geophys. Res. D Atmos.*, vol. 108, no. 17, pp. 1–15, 2003

[22] J. Yoram Kaufman, "Aerosol Optical Thickness and Atmospheric Path Radiance," *Geophys. Res. Lett.*, vol. 98, no. 2, pp. 2677–2692, 1993.

[23] T. F. Eck, B. N. Holben, A. Smirnov, I. Slutsker, J. M. Lobert, and V. Ramanathan, "Column-integrated aerosol optical properties over the Maidives during the northeast," *Geophys. Res. Lett.*, vol. 106, no. 22, pp. 28555–28566, 2001.

[24] J. S. Reid, A. Smirnov, N. T. O. Neill, I. Slutsker, and S. Kinne, "Wavelength dependence of the optical depth of biomass burning, urban, and desert aerosols," *Geophys. Res.*, vol. 104, no. 1, pp. 31333–31349, 1999.

[25] T. F. Eck *et al.*, "Characterization of the optical properties of biomass burning aerosols in Zambia during the 1997 ZIBBEE field campaign," *Geophys. Res.*, vol. 106, no. 4, pp. 3425–3448, 2001.

[26] B. I. Tijjani, "The Effect of Soot and Water Soluble on the Hygroscopicity of Urban Aerosols," *Adv. Phys. Theor. Appl.*, vol. 26, no. 1, pp. 52–73, 2013

[27] P. K. Quinn *et al.*, "Impact of particulate organic matter on the relative humidity dependence of light scattering: A simplified parameterization," *Geophys. Res. Lett.*, vol. 32, no. 22, pp. 1–4, 2005

[28] Junge et. al., "Chapter 2 Physical and Optical properties of aerosols," *Geophys. Res. Lett.*, vol. 1, no. 1, pp. 220–247, 1958.

[29] S. Sjogren, M. Gysel, E. Weingartner, U. Baltensperger, M. J. Cubison, and H. Coe, "Hygroscopic growth and water uptake kinetics of two-phase aerosol particles consisting of ammonium sulfate , adipic and humic acid mixtures," *Aerosol Sci.*, vol. 38, no. 1, pp. 157–171, 2007

[30] E. Swietlicki *et al.*, "Hygroscopic properties of submicrometer atmospheric aerosol particles measured with H-TDMA instruments in various environments - A review," *Tellus, Ser. B Chem. Phys. Meteorol.*, vol. 60 B, no. 3, pp. 432–469, 2008